Crystal structure and ferroelectric properties of $A\mathrm{Bi_2Ta_2O_9}$ (A=Ca, Sr, and Ba)

Y. Shimakawa and Y. Kubo
Fundamental Research Laboratories, NEC Corporation, 34 Miyukigaoka, Tsukuba 305-8501, Japan

Y. Nakagawa, S. Goto, T. Kamiyama, and H. Asano
Institute for Materials Science, University of Tsukuba, 1-1-1 Tennodai, Tsukuba 305-8577, Japan

F. Izumi
National Institute for Research in Inorganic Materials, 1-1 Namiki, Tsukuba 305-0044, Japan

(Received 28 July 1999)

Crystal structures and ferroelectric properties of a series of Bi-layered compounds, $\mathrm{CaBi_2Ta_2O_9}$, $\mathrm{SrBi_2Ta_2O_9}$, and $\mathrm{BaBi_2Ta_2O_9}$, were investigated. The structures of $\mathrm{CaBi_2Ta_2O_9}$ and $\mathrm{SrBi_2Ta_2O_9}$ are orthorhombic, while that of $\mathrm{BaBi_2Ta_2O_9}$ is pseudotetragonal on the macroscopic scale but consists of microdomains with orthorhombic distortion. The ferroelectric Curie temperature of $\mathrm{CaBi_2Ta_2O_9}$ was over 600 °C, and that of $\mathrm{SrBi_2Ta_2O_9}$ was over 300 °C. $\mathrm{BaBi_2Ta_2O_9}$, in contrast, showed relaxor-type ferroelectric behavior; that is, in the plot of temperature dependence of dielectric constant, a broad peak appeared around 60 °C. As the size of the A-site cation decreases from $\mathrm{Ba^{2+}}$ to $\mathrm{Ca^{2+}}$, the lattice mismatch between $\mathrm{TaO_2}$ and AO planes in the perovskite-type unit of $A\mathrm{Ta_2O_7}$ increases and the structural distortion becomes more pronounced. This distortion leads to the higher Curie temperature and the larger spontaneous ferroelectric polarization.

I. INTRODUCTION

In recent years ferroelectric thin films have attracted a lot of attention for use in nonvolatile memory applications (ferroelectric random access memories). Bi-layered compounds as well as $\mathrm{PbZr_{1-x}Ti_xO_3}$ perovskites are leading candidates for such devices and have been extensively studied. These so-called Aurivillius compounds were discovered in the late 40's,[1–3] and their basic structural and ferroelectric properties were studied in the early 60's.[4] Among these compounds, ferroelectric $\mathrm{SrBi_2Ta_2O_9}$ has been the most intensively studied for use in memory devices due to its fatigue-free nature.[5,6]

The crystal structure of $\mathrm{SrBi_2Ta_2O_9}$ consists of $\mathrm{Bi_2O_2}$ layers and perovskite-type $\mathrm{SrTa_2O_7}$ units with double $\mathrm{TaO_6}$ octahedral layers. And it was studied by using neutron and electron diffraction, which revealed orthorhombic distortion with space group $A2_1am$.[7,8] The structural distortion with this noncentrosymmetric space group is responsible for the displacive-type ferroelectric behavior of the compound; that is, atomic displacements along the a axis from corresponding positions in the parent tetragonal ($I4/mmm$) structure cause spontaneous ferroelectric polarization.

We previously studied crystal structures of stoichiometric $\mathrm{SrBi_2Ta_2O_9}$ and off-stoichiometric $\mathrm{Sr_{0.8}Bi_{2.2}Ta_2O_9}$ ferroelectric materials by neutron powder diffraction and revealed that cation substitution at a Sr site significantly influences ferroelectric properties.[9] In the off-stoichiometric sample, both Bi substitution and cation vacancies exist at the Sr site, and chemical composition of the material is $(\mathrm{Sr_{0.82}Bi_{0.12}})\mathrm{Bi_2Ta_2O_{9.0}}$. The substitution of smaller $\mathrm{Bi^{3+}}$ for $\mathrm{Sr^{2+}}$ increases structural distortion, which leads to larger ferroelectric polarization and higher ferroelectric Curie temperature. This finding suggested that the size of the A-site cation strongly affects ferroelectric properties.

In the present work, we have analyzed the crystal structures of a series of Bi-layered compounds with different A-site cations, i.e., $A\mathrm{Bi_2Ta_2O_9}$ (A=Ca, Sr, and Ba). High-resolution neutron powder diffraction can reveal the detailed crystal structures of such displacive-type ferroelectric materials. We are thus able to understand the relationships between crystal structures and ferroelectric properties. Consequently, we have found that the structural distortion increases with decreasing size of the A-site cation and that ferroelectric properties are strongly affected by structural distortion.

II. EXPERIMENTS

Powder samples of $\mathrm{CaBi_2Ta_2O_9}$, $\mathrm{SrBi_2Ta_2O_9}$, and $\mathrm{BaBi_2Ta_2O_9}$ were prepared by solid-state reaction. Mixtures of appropriate amounts of $\mathrm{CaCO_3}$, $\mathrm{SrCO_3}$, $\mathrm{BaCO_3}$, $\mathrm{Bi_2O_3}$, and $\mathrm{Ta_2O_5}$ were sintered at 1000–1370 °C for 12–30 h in air. The samples were confirmed to be single phases by both x-ray and neutron diffraction. Capacitance of the disk-shaped samples was measured at temperatures from −180 to 600 °C by using a conventional LCR meter with a frequency of 1, 10, and 100 kHz. The P (polarization)-E (electric field) hysteresis loop was measured at room temperature by a Sawyer-Tower circuit. Time-of-flight neutron powder diffraction data were collected at room temperature on the Vega diffractometer at KENS.[10] Structural parameters were refined by the Rietveld method with the program RIETAN-98T.[11] A structural change of $\mathrm{BaBi_2Ta_2O_9}$ at low temperature was investigated by x-ray diffraction. The measurements were carried out at temperatures from room temperature down to −250 °C by using θ-2θ goniometer equipped with a refrigerator.

III. RESULTS

The x-ray and neutron-diffraction patterns showed that structures of $\mathrm{CaBi_2Ta_2O_9}$ and $\mathrm{SrBi_2Ta_2O_9}$ are orthorhombic

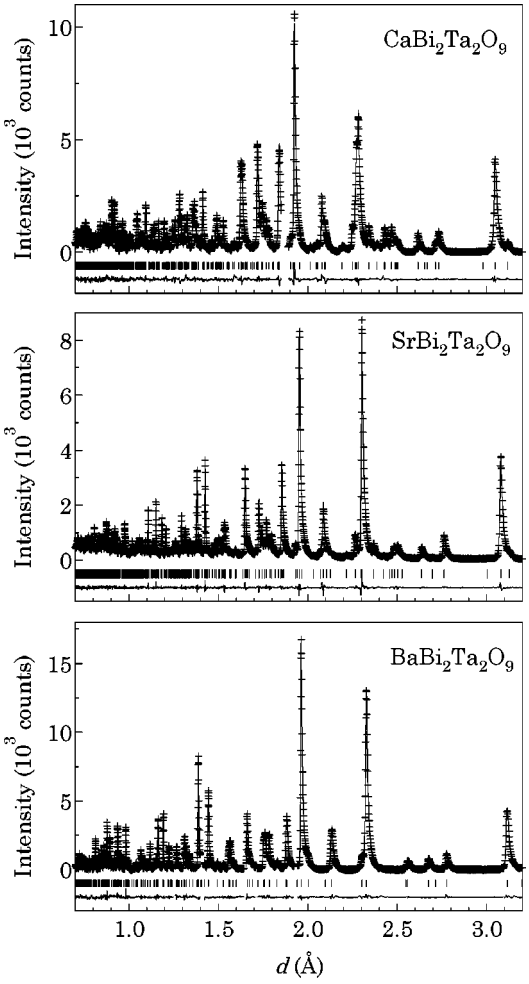

FIG. 1. Neutron-diffraction patterns of $ABi_2Ta_2O_9$ (A=Ca, Sr, and Ba) and the Rietveld refinement profiles. The observed diffraction data are shown as plus marks, and the calculated profile as a solid line. Tick marks below the profile mark the positions of allowed reflections. Differences between the observed and the calculated intensities are shown at the bottom.

with space group $A2_1am$. No anomalous occupancies were observed at any of the sites, which provides evidence for stoichiometric compositions as expected from the nominal ones. However, structural refinement of $BaBi_2Ta_2O_9$ with the orthorhombic $A2_1am$ space group was unsuccessful. Attempts to refine structural parameters on the basis of the orthorhombic cell resulted in convergence to a pseudotetragonal ($a \approx b$) structure. In addition, characteristic orthorhombic reflections such as 1 2 2 ($d \approx 2.41$ Å) and 5 1 2 ($d \approx 2.20$ Å) are extinct in $BaBi_2Ta_2O_9$. Since these reflections are not allowed in the tetragonal symmetry, the diffraction data support the pseudotetragonal structure of $BaBi_2Ta_2O_9$. Then, structural parameters of $BaBi_2Ta_2O_9$ were refined according to a pseudotetragonal cell with space group $I4/mmm$. Observed reflections of $BaBi_2Ta_2O_9$ showed considerable anisotropic broadening, which was corrected by using partial profile relaxation.[11] Figure 1 shows the neutron powder diffraction patterns at room temperature and Rietveld refinement profiles for the three samples. Tables I, II, and III list the refined structural parameters of each compound.

The thermal parameter of the Bi site in $BaBi_2Ta_2O_9$ (B_{eq}=2.70 Å^2) is much larger than those in $CaBi_2Ta_2O_9$ (1.00 Å^2) and $SrBi_2Ta_2O_9$ (1.54 Å^2). This result might indicate a mutual substitution between the Ba and Bi ions, as reported in isostructural $BaBi_2Nb_2O_9$.[12] The refinement according to a model with Ba and Bi substitutions at the Bi and Ba sites, respectively, slightly lowered R_{wp} from 4.79 to 4.67%, but the refined thermal parameter of the Bi site increased from 2.70 to 2.90 Å^2. Thus, we could not confirm such substitution. Because the resulting positional parameters of $BaBi_2Ta_2O_9$ were practically identical in both models, we focus only on positional parameters of $BaBi_2Ta_2O_9$ in the present study.

Figure 2 shows the temperature dependence of the dielectric constant, ε, of the three $ABi_2Ta_2O_9$ samples. $SrBi_2Ta_2O_9$ exhibited typical ferroelectric behavior with a ferroelectric Curie temperature (T_C) of 300 °C. The dielectric constant above T_C obeyed the Curie-Weiss law. And the dielectric constant of $CaBi_2Ta_2O_9$ gradually increased with increasing temperature but did not show a transition peak up to 600 °C. The measurement of ε above 600 °C was, however, unsuccessful because dielectric loss increased owing to a conducting property of the sample. Since the ferroelectric state of $CaBi_2Ta_2O_9$ at room temperature was confirmed by a P-E hysteresis measurement, the Curie temperature of $CaBi_2Ta_2O_9$ should be over 600 °C. In the plot of ε against

TABLE I. Refined structural parameters of $CaBi_2Ta_2O_9$. Numbers in parentheses are standard deviations of the last significant digit. B_{eq} is the equivalent isotropic thermal parameter obtained from refined anisotropic thermal parameters. No vacancies were detected at all the sites, and, therefore, all the occupation factors were fixed at 1. Space group; $A2_1am$. a=5.4625(1) Å, b=5.4286(1) Å, and c=24.9450(6) Å. R_{wp}=3.70%, R_p=2.82%, R_I=0.80%, R_F=0.54%, and R_e=2.79%.

Atom	Position	x	y	z	g	B_{eq} (Å^2)
Ca	4a	0	0.2484(11)	0	1	0.43
Bi	8b	0.4865(15)	0.7749(4)	0.198 94(8)	1	1.00
Ta	8b	0.5285(15)	0.7510(7)	0.416 80(7)	1	0.10
O(1)	4a	0.5575(19)	0.3175(10)	0	1	0.98
O(2)	8b	0.5299(17)	0.6800(7)	0.344 39(11)	1	0.90
O(3)	8b	0.7535(16)	0.9952(9)	0.250 25(15)	1	0.84
O(4)	8b	0.7555(17)	0.9638(8)	0.063 89(14)	1	0.59
O(5)	8b	0.8423(14)	0.9490(8)	0.585 78(16)	1	0.94

TABLE II. Refined structural parameters of $SrBi_2Ta_2O_9$: Space group; $A2_1am$. $a=5.5224(2)$ Å, $b=5.5241(2)$ Å, and $c=25.0264(5)$ Å. $R_{wp}=4.90\%$, $R_p=3.73\%$, $R_I=1.37\%$, $R_F=1.03\%$, and $R_e=4.64\%$.

Atom	Position	x	y	z	g	B_{eq} (Å^2)
Sr	4a	0	0.2567(9)	0	1	0.69
Bi	8b	0.4634(8)	0.7764(6)	0.199 96(7)	1	1.54
Ta	8b	0.5104(13)	0.7480(7)	0.414 82(7)	1	0.39
O(1)	4a	0.5248(14)	0.2892(13)	0	1	1.04
O(2)	8b	0.5219(12)	0.6990(11)	0.341 87(11)	1	1.55
O(3)	8b	0.7381(13)	0.9923(8)	0.250 76(13)	1	0.85
O(4)	8b	0.7554(14)	0.9867(8)	0.069 64(10)	1	0.62
O(5)	8b	0.7909(12)	0.9807(8)	0.583 59(11)	1	0.91

temperature in $BaBi_2Ta_2O_9$, there was a broad maximum around 60 °C. In addition, ε significantly depended on measured frequency. The P-E measurement at room temperature did not show an apparent ferroelectric hysteresis loop.

Apparent orthorhombic distortion in $BaBi_2Ta_2O_9$ was not observed even at low temperatures. X-ray diffraction peaks measured at −250 °C could be indexed on the basis of the pseudotetragonal cell. Both the full width at half maximum of the 1 1 0 reflection and the intensity ratio of $I(1\ 1\ 0)/I(0\ 0\ 10)$ remained unchanged over the measured temperature range. (The 1 1 0 reflection in the tetragonal structure should split into two peaks in the orthorhombic structure.) As shown in Fig. 3, no anomalous changes were observed in the plots of lattice parameters a and c against temperature. The lattice parameters c decreased smoothly by about −0.19% over the measured temperature range, but a decreased only slightly by about −0.03%.

IV. DISCUSSION

We first discuss the structural and ferroelectric properties of $BaBi_2Ta_2O_9$. The refined crystal structure of $BaBi_2Ta_2O_9$ resulted in a pseudotetragonal cell without apparent displacive orthorhombic distortion. Further, no ferroelectric polarization was found in the P-E hysteresis measurement at room temperature. However, the temperature dependence of the dielectric constant showed the broad peak around 60 °C, suggesting a ferroelectric transition. This kind of broad transition peaks in ε are often observed in relaxor-type ferroelectric materials such as $PbMg_{1/3}Nb_{2/3}O_3$.[13] In these materials, microscopic ferroelectric domains have slightly different T_C values, which cause gradual ferroelectric transition as indicated by the broad peak in the plot of temperature dependence of dielectric constant. The significant frequency dependence of ε is also a characteristic feature of the relaxor-type ferroelectrics. It is, therefore, reasonable to conclude that the observed broad peak in ε of $BaBi_2Ta_2O_9$ corresponds to a relaxor-type ferroelectric transition. The transition temperature quite close to room temperature appears to explain why no apparent ferroelectric hysteresis loop was observed at room temperature.

The diffraction pattern of $BaBi_2Ta_2O_9$ exhibiting the pseudotetragonal unit cell must reflect the ''averaged'' structure; that is, the $BaBi_2Ta_2O_9$ structure consists of microdomains with orthorhombic distortion, which causes the relaxor-type ferroelectric transition. The anisotropic peak broadening and the large thermal parameters revealed in the structure refinement based on the macroscopic $I4/mmm$ tetragonal symmetry also result from the microscopic structural distortion.

We next discuss structural features of $ABi_2Ta_2O_9$. As shown in Fig. 4, lattice parameters increased as the size of the A-site cation increased. Orthorhombicity, $2(a-b)/(a+b)$, decreased with increasing size of the A-site cation. The structural distortion is explained in terms of a lattice mismatch between TaO_2 and AO planes in the perovskite-type unit of ATa_2O_7. In a purely ionic model, tolerance factor, t, for the perovskite structure is given by

$$t=(r_A+r_O)/\sqrt{2}(r_B+r_O), \tag{1}$$

TABLE III. Refined structural parameters of $BaBi_2Ta_2O_9$: Space group; $I4/mmm$. $a=3.926\,50(8)$ Å and $c=25.5866(8)$ Å. $R_{wp}=4.79\%$, $R_p=3.55\%$, $R_I=1.93\%$, $R_F=1.85\%$, and $R_e=2.93\%$.

Atom	Position	x	y	z	g	B_{eq} (Å^2)
Ba	2a	0	0	0	1 [a]	0.85
Bi	4e	0	0	0.201 87(19)	1 [a]	2.70
Ta	4e	0	0	0.412 00(13)	1	0.31
O(1)	2b	0	0	1/2	1	1.45
O(2)	4e	0	0	0.340 32(18)	1	2.30
O(3)	4d	0	1/2	1/4	1	0.93
O(4)	8g	0	1/2	0.421 27(14)	1	0.99

[a]Substitution between Ba and Bi ions might occur (see text).

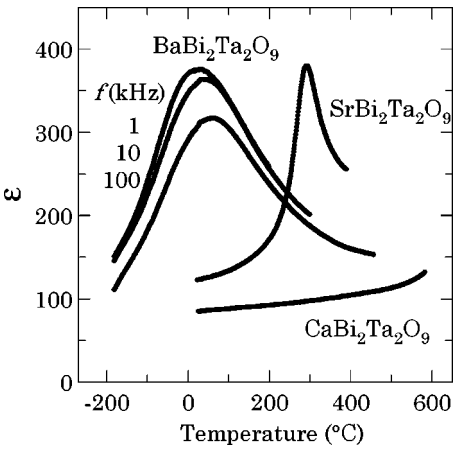

FIG. 2. Temperature dependence of the dielectric constant ε of $ABi_2Ta_2O_9$ (A=Ca, Sr, and Ba). The data of $BaBi_2Ta_2O_9$ measured with different frequencies from 1 to 100 kHz are also shown.

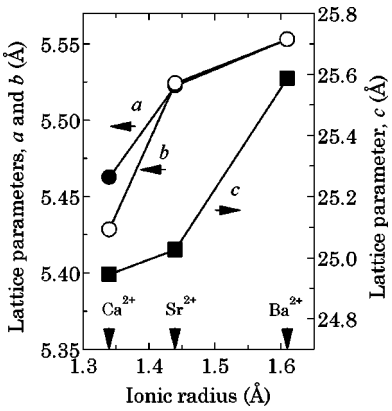

FIG. 4. Lattice parameters of $ABi_2Ta_2O_9$ (A=Ca, Sr, and Ba) plotted against the ionic radii of the A^{2+} ions. The pseudotetragonal lattice parameters of $BaBi_2Ta_2O_9$ were converted to the orthorhombic ones.

where r_A, r_B, and r_O are ionic radii of an A-site cation, a B-site cation, and an oxygen ion, respectively.[14] If we apply this relation to the perovskite-type unit of $ABi_2Ta_2O_9$, the tolerance factors are those listed in Table IV. Note that t's of orthorhombic $CaBi_2Ta_2O_9$ and $SrBi_2Ta_2O_9$ are less than 1 while t of pseudotetragonal $BaBi_2Ta_2O_9$ is more than unity. This means that, in the orthorhombic structure, the TaO_2 plane is under compressive stress while the AO plane is under tensile stress. This type of lattice mismatch usually causes cooperative rotations of BO_6 octahedra, i.e., $GdFeO_3$-type distortion. In the Bi-layered compounds, however, such cooperative rotations of the octahedra are not allowed owing to the presence of the Bi_2O_2 layers above and below the ATa_2O_7 perovskite-type unit: thus, the octahedron itself is considerably distorted, leading to the $A2_1am$ orthorhombic symmetry.

Figure 5 illustrates the crystal structures of $ABi_2Ta_2O_9$ as projections onto a-b and a-c planes in the orthorhombic cell. The structures were drawn with the refined positional parameters listed in Tables I, II, and III. As clearly seen in the figure, the distortion of the TaO_6 octahedra becomes more pronounced as the size of the A-site cation decreases. Table V lists the selected bond lengths and angles of the TaO_6 octahedra and the Bi_2O_2 layers. Four different Ta-O bond lengths in the TaO_2 plane are included in orthorhombic $CaBi_2Ta_2O_9$ and $SrBi_2Ta_2O_9$, though these bonds are equivalent in pseudotetragonal $BaBi_2Ta_2O_9$. The lengths of these bonds lie between 1.921(6) and 2.049(6) Å in $CaBi_2Ta_2O_9$ and between 1.928(5) and 2.017(5) Å in $SrBi_2Ta_2O_9$. The difference in the lengths of the longest [one of the Ta-O(4) bonds] and the shortest [one of the Ta-O(5) bonds] bonds is larger in $CaBi_2Ta_2O_9$ than that in $SrBi_2Ta_2O_9$. This finding reveals the octahedra in $CaBi_2Ta_2O_9$ to be more distorted. The TaO_6 octahedra are buckled along the b axis in the orthorhombic Ca and Sr systems. The tilting angles of the octahedra from the c axis obtained from the bond angles of Ta-O(1)-Ta are 10.8(3)° ($CaBi_2Ta_2O_9$), 6.5(3)° ($SrBi_2Ta_2O_9$), and 0° ($BaBi_2Ta_2O_9$). Therefore, $CaBi_2Ta_2O_9$ is the most structurally distorted. Since the lattice mismatch between the TaO_2 and AO planes in the octahedral unit of $CaBi_2Ta_2O_9$ is expected to be the most pronounced among the three $ABi_2Ta_2O_9$ compounds as indicated by the smallest t value, the observed largest distortion of the octahedra in $CaBi_2Ta_2O_9$ is quite reasonable.

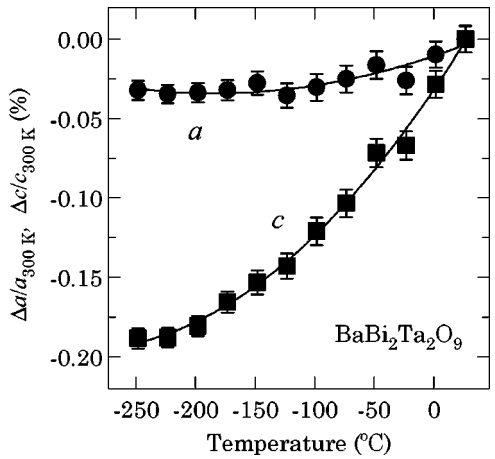

FIG. 3. Changes in the lattice parameters of $BaBi_2Ta_2O_9$ at low temperatures.

In the $A2_1am$ orthorhombic structure, atomic displacements along the a axis from the corresponding positions in the parent tetragonal structure produce spontaneous ferroelectric polarization. By setting the position of the A site at the origin, Fig 6(a), illustrates atomic displacements along the a axis of each constituent ion in $CaBi_2Ta_2O_9$ and $SrBi_2Ta_2O_9$. No ions in pseudotetragonal $BaBi_2Ta_2O_9$ are displaced in such ways; thus, the positions of the ions are

TABLE IV. Ionic radii (Å) of A^{2+} ions coordinated to 12 oxygen ions and tolerance factors, t, for the ATa_2O_7 perovskite-type units. Ionic radii of Ta^{5+} coordinated to 6 oxygen ions and O^{2-} are 0.64 and 1.40 Å , respectively.

	Ca	Sr	Ba
ionic radius	1.34	1.44	1.61
t	0.95	0.98	1.04

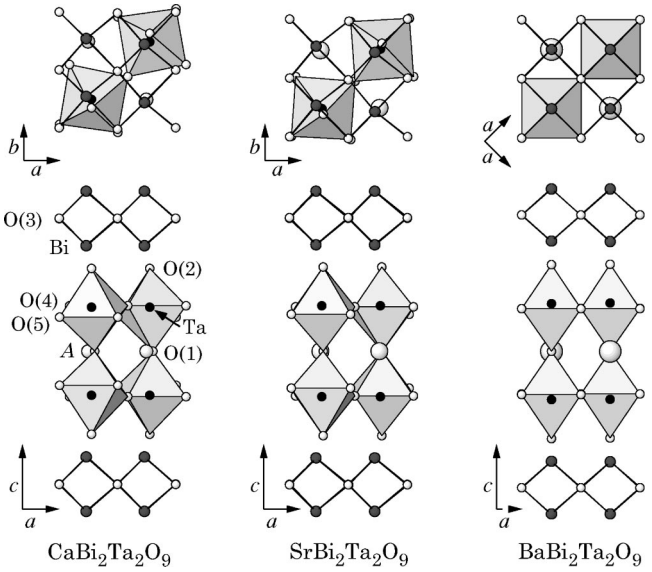

FIG. 5. Crystal structures of $ABi_2Ta_2O_9$ (A=Ca, Sr, and Ba) drawn with the positional parameters refined with the neutron-diffraction data.

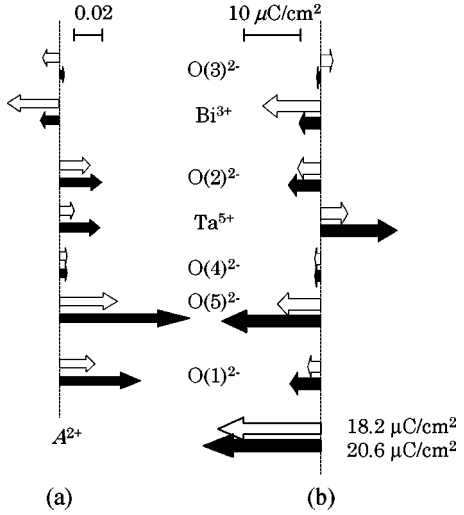

FIG. 6. Schematic drawings of (a) atomic displacements (fraction of the a axis length) and (b) contributions to the total ferroelectric polarization ($\mu C/cm^2$) of each ion of $CaBi_2Ta_2O_9$ (closed arrows) and $SrBi_2Ta_2O_9$ (open arrows). The position of the A site on the a axis is fixed at the origin.

located on a solid line in the center. The displacements along the a axis in the orthorhombic structure show that the Bi_2O_2 layers and the ATa_2O_7 perovskite-type units shift in opposite directions. It is notable that the ions, particularly Ta^{5+}, $O(1)^{2-}$, and $O(5)^{2-}$ in the ATa_2O_7 unit of $CaBi_2Ta_2O_9$, are more displaced than those of $SrBi_2Ta_2O_9$. The Bi^{3+} ion in the Bi_2O_2 layer, on the other hand, is more displaced in $SrBi_2Ta_2O_9$.

From the atomic displacements, we can calculate the total polarization of the displacive-type ferroelectric $CaBi_2Ta_2O_9$ and $SrBi_2Ta_2O_9$ as

$$P_s=\Sigma_i(m_i\times\Delta x_i\times Q_ie)/V, \tag{2}$$

where m_i is the site multiplicity, Δx_i is the atomic displacement along the a axis from the corresponding position in the tetragonal structure, Q_ie is the ionic charge of the ith constituent ion, and V is the unit-cell volume. The contributions of each constituent ion to the total ferroelectric polarization are shown in Fig. 6(b). The polarizations of $CaBi_2Ta_2O_9$ and $SrBi_2Ta_2O_9$ were calculated at 20.6 and 18.2 $\mu C/cm^2$, respectively. In $CaBi_2Ta_2O_9$, the large atomic displacement of the $O(5)^{2-}$ ion in the TaO_6 octahedron plays a major role in the marked ferroelectric polarization. The large atomic displacement of the Bi^{3+} ion also contributes greatly to the spontaneous ferroelectric polarization of $SrBi_2Ta_2O_9$.

TABLE V. Selected bond lengths (Å) and angles (°) of $ABi_2Ta_2O_9$ (A=Ca, Sr, and Ba).

	$CaBi_2Ta_2O_9$	$SrBi_2Ta_2O_9$	$BaBi_2Ta_2O_9$
Bi-O(3)	2.280(6)	2.311(4)	2.317(2) (×4)
	2.194(6)	2.190(4)	
	2.458(6)	2.507(4)	
	2.318(6)	2.296(4)	
Ta-O(1)	2.113(2)	2.145(2)	2.256(3)
Ta-O(2)	1.847(3)	1.847(3)	1.822(6)
Ta-O(4)	1.954(7)	1.953(5)	1.9786(6) (×4)
	2.049(6)	2.017(5)	
Ta-O(5)	1.921(6)	1.928(5)	
	2.024(6)	2.013(5)	
Ta-O(1)-Ta	158.5(3)	167.1(3)	180
TaO_6 tilting	10.8	6.5	0

V. SUMMARY

We synthesized a series of Bi-layered compounds, $CaBi_2Ta_2O_9$, $SrBi_2Ta_2O_9$, and $BaBi_2Ta_2O_9$, and examined their crystal structures and ferroelectric properties. The structure analysis by neutron diffraction revealed that the structures of ferroelectric $CaBi_2Ta_2O_9$ ($T_C>600\,°C$) and $SrBi_2Ta_2O_9$ ($T_C=300\,°C$) are orthorhombic with the $A2_1am$ symmetry, whereas that of $BaBi_2Ta_2O_9$ is pseudotetragonal ($I4/mmm$). The macroscopic pseudotetragonal structure of $BaBi_2Ta_2O_9$ consists of microdomains with orthorhombic distortion, which causes the relaxor-type ferroelectric transition around 60 °C. The structural distortion is well explained in terms of the lattice mismatch between the TaO_2 and AO planes, where the mismatch is estimated by the tolerance factor for the perovskite-type unit. As the size of the A-site cation decreases from Ba^{2+} to Ca^{2+}, the lattice mismatch increases (t decreases), and the structural distortion becomes more pronounced. This pronounced distortion leads to the higher Curie temperature and the larger spontaneous ferroelectric polarization. This finding is consistent with our previous observation in the stoichiometric $SrBi_2Ta_2O_9$ and the off-stoichiometric $Sr_{0.8}Bi_{2.2}Ta_2O_9$; that is, substitution of smaller Bi^{3+} ions for Sr^{2+} ions at the Sr site increases structural distortion, leading to larger ferroelectric polarization and higher ferroelectric Curie temperature.

[1] B. Aurivillius, Ark. Kemi **1**, 463 (1949).
[2] B. Aurivillius, Ark. Kemi **1**, 499 (1949).
[3] B. Aurivillius, Ark. Kemi **2**, 519 (1950).
[4] E. C. Subbarao, J. Phys. Chem. Solids **23**, 665 (1962).
[5] C. A-Paz de Araujo, J. D. Cuchiaro, L. D. McMillan, M. C. Scott, and J. F. Scott, Nature (London) **374**, 627 (1995).
[6] K. Amanuma, T. Hase, and Y. Miyasaka, Appl. Phys. Lett. **66**, 221 (1995).
[7] R. E. Newnham, R. W. Wolfe, R. S. Horsey, F. A. Diaz-Colon, and M. I. Kay, Mater. Res. Bull. **8**, 1183 (1973).
[8] A. D. Rae, J. G. Thompson, and R. L. Withers, Acta Crystallogr., Sect. B: Struct. Sci. **48**, 418 (1992).
[9] Y. Shimakawa, Y. Kubo, Y. Nakagawa, T. Kamiyama, H. Asano, and F. Izumi, Appl. Phys. Lett. **74**, 1904 (1999).
[10] T. Kamiyama, K. Oikawa, N. Tsuchiya, M. Osawa, H. Asano, N. Watanabe, M. Furusaka, S. Satoh, I. Fujikawa, T. Ishigaki, and F. Izumi, Physica B **213-214**, 875 (1995).
[11] T. Ohta, F. Izumi, K. Oikawa, and T. Kamiyama, Physica B **234-236**, 1093 (1997).
[12] S. M. Blake, M. J. Falconer, M. MaCreedy, and P. Lightfoot, J. Mater. Chem. **7**, 1609 (1997).
[13] Z. G. Lu and G. Galvarin, Phys. Rev. B **51**, 2694 (1995).
[14] For ionic radii, see R. D. Shannon, Acta Crystallogr., Sect. A: Cryst. Phys., Diffr., Theor. Gen. Crystallogr. **A32**, 751 (1976).